Particle Accelerators, 1971, Vol. 2, pp. 57–68

EFFECTS OF MAGNETIC LENS ABERRATION IN HIGH-CURRENT LINEAR ACCELERATORS†

C. H. WOODS AND R. P. FREIS

Lawrence Radiation Laboratory, University of California, Livermore, California, U.S.A.

The geometrical aberration inherent in several different magnetic lens structures is calculated and compared. Two of these satisfy our definition of a thin lens. We consider beam transport through perfect and imperfect lenses, and we show that beams can be compensated by adjusting the radial density distribution to match the lens aberration. Finally, we show that uncompensated high-current beams may become hollow through self interaction.

1. INTRODUCTION

There is increasing interest in high-current electron accelerators for producing x-rays,[1] injecting relativistic electrons into thermonuclear devices[2] (Astron), and fundamental beam-plasma researches.[3] Beams of the order of 10^6 amperes and a few MeV energy can be produced by simply driving a cathode negative to the required potential and allowing the electrons to pass through a thin anode. Where it is desirable to increase the energy further than this, or where control of the beam quality (phase-space distribution) is important, induction-type accelerators can be employed. Axially symmetric focusing magnets can be used to transport circular beams through an indefinite number of accelerator stages, and in principle there is no limit to the beam energy that can be achieved.

Good performance of a high-current accelerator is dependent on careful placement of the focusing magnets and correct settings for the focal lengths, with due consideration of image effects in the accelerator sections between the magnets.[4] The quality of these magnetic 'lenses' is also an important factor, which we will consider in some detail.

2. BEAM TRANSPORT THROUGH PERFECT LENSES

Ideally a magnetic lens for this purpose should perform like a thin convex optical lens, i.e., it should focus parallel single-particle rays to a common point. In high-current devices the particles interact collectively to produce radial beam expansion, and focusing must be introduced at frequent intervals (or continuously) along the axis to control the beam size. Let us consider how to set up a circular coasting beam in laminar flow. The axial electric field will be neglected because it adds a parameter to the problem which is not especially relevant in considering the effects of lens aberration.

We arrange for a periodic beam envelope in the interval $-\infty < z < \infty$ by placing a perfect lens at each of the points $z = \pm Z/2, \pm 3Z/2, \pm 5Z/2, \ldots$, where Z is the interval between lenses. The particles in a high-current (unneutralized) beam are always accelerated outward radially (r, θ, z) except where they are passing through a lens. Through the proper choice of the lens focal length and the interval Z, it is possible to set up a periodic beam of variable radius $R(z)$ having minima $R = R_{\min}$ at $z = 0, \pm Z, \pm 2Z, \ldots$, and maxima $R = R_{\max}$ at the lens locations. The required lens parameters can be determined for the laminar flow by integrating the equation[5]

$$\mathrm{d}^2R/\mathrm{d}z^2 = A^2/R \tag{1}$$

for the beam envelope, where

$$A^2 = 2Iq/m_0c^2\beta^3\gamma^3, \tag{2}$$

is a dimensionless flow amplitude proportional to the total beam current I, q is the particle charge ($q = -e$ for electrons), and the other symbols have their usual meanings. The constant A^2 takes account of the electric and magnetic fields produced by the beam. Integrating Eq. (1), we have

$$\mathrm{d}R/\mathrm{d}z = A(2\ln R/R_{\min})^{1/2} \tag{3}$$

and

$$z = (\sqrt{2}\,R_{\min}/A)\int_0^{\sqrt{\ln R/R_{\min}}} \exp(t^2)\,\mathrm{d}t. \tag{4}$$

A periodic envelope is realized by setting

$$z = Z/2 \tag{5}$$

$$R = R_{\max} \tag{6}$$

† Work performed under the auspices of the U.S. Atomic Energy Commission.

and

$$2\,dR/dz = R_{max}/f \tag{7}$$

where the factor 2 appears in the last equation because each lens is required to focus inward ($-dR/dz$) a beam which is already expanding at the same rate ($+dR/dz$). Equation (7) assumes that the change in slope of the beam envelope on passing through the lens is R_{max}/f. Because of this linear dependence on R_{max}, the lens is said to be linear, perfect, and free of aberration. In the next section we shall see that in magnetic lenses f generally depends to some extent on R_{max}, so that proportionality is lost, and the lens is said to be nonlinear.

To simplify the equations, let

$$\alpha = (\ln R_{max}/R_{min})^{1/2} = (\ln \mu)^{1/2} \tag{8}$$

and

$$\Phi(\alpha) = \int_0^\alpha \exp(t^2)\,dt. \tag{9}$$

If we now substitute Eq. (7) into Eq. (3), multiply by Eq. (4), and then make the substitutions indicated in Eqs. (5) and (6), we obtain the equation

$$Z/f = 8\alpha \exp(-\alpha^2)\Phi(\alpha), \tag{10}$$

which is a necessary condition for a periodic coasting beam. This ratio of lens spacing to focal length is plotted versus R_{max}/R_{min} in Fig. 1. It should be noted that Eq. (10) is independent of A.

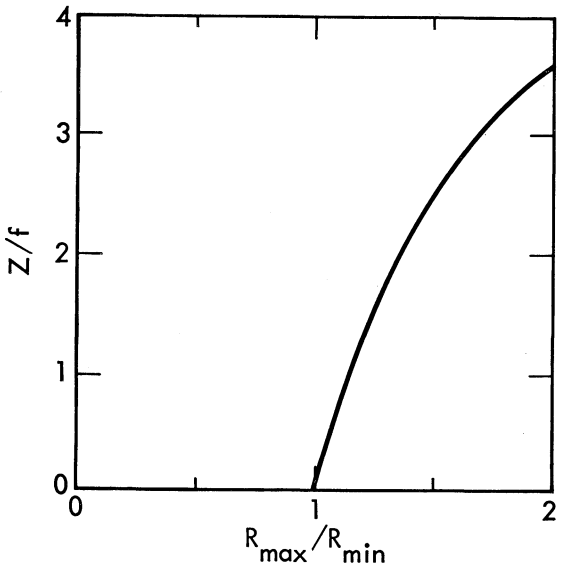

FIG. 1. Curve showing combinations of lens parameters and beam parameters which produce a periodic, time-independent structure.

The procedure for determining the lens parameters is first to select a value of $\mu = R_{max}/R_{min}$, which allows determination of Z/f from Eq. (10), or from Fig. 1. The next step is to select the beam radius, which then allows determination of the required focal length from the equation

$$f = \frac{\sqrt{2}\,R_{max}}{4\alpha A}, \tag{11}$$

found by substituting Eq. (7) into Eq. (3), and which is a second necessary condition for periodic flow.

In practice the maximum beam radius is usually chosen to be only 10 to 20 per cent larger than the minimum radius. From Fig. 1 it is apparent that for a typical case, say $\mu = R_{max}/R_{min} = 1.15$, the value of Z/f is approximately unity. Thus the required focal length and lens interval are usually comparable.

3. ABERRATION IN TYPICAL LENSES

We turn now to a determination of the focusing properties of typical real magnetic lenses. Almost any axially symmetric magnetic field ($B_r\hat{r} + B_z\hat{z}$) localized in space and produced by an axially symmetric source outside the beam will form a lens. For example, a current ring, a long or short solenoid, or a current ring partially clad with iron will focus a beam passing through it.

We can see at once how a symmetric magnetic lens is able to focus particles. The only component of the vector magnetic potential is $A_\theta(r, z)$, and the relativistic Hamiltonian

$$H = \left\{c^2\left[p_r^2 + \frac{1}{r^2}\left(p_\theta - \frac{q}{c}rA_\theta\right)^2 + p_z^2\right] + m_0^2c^4\right\}^{1/2} \tag{12}$$

rewritten in the form

$$\frac{H^2 - m_0^2c^4}{2\gamma m_0 c^2} = \frac{p_r^2}{2\gamma m_0} + \frac{p_z^2}{2\gamma m_0} + \frac{1}{2\gamma m_0 r^2}\left(p_\theta - \frac{q}{c}rA_\theta\right)^2 \tag{13}$$

suggests a new nonrelativistic Hamiltonian

$$H^* = T + V \tag{14}$$

in which

$$H^* = \frac{H^2 - m_0c^4}{2\gamma m_0 c^2} \tag{15}$$

and

$$V(r, z) = \frac{1}{2\gamma m_0 r^2}\left[p_\theta - \frac{q}{c}rA_\theta(r, z)\right]^2 \tag{16}$$

where the mass γm_0 and the canonical momentum p_θ are constants of the motion. In the lens problem

we consider the trajectory of a particle coming initially from $z = -\infty$ moving parallel to the z-axis, with $p_r = 0$, and p_z positive. The potential A_θ vanishes at $z = \pm\infty$, and consequently $p_\theta = 0$, and

$$V(r, z) = \frac{q^2}{2\gamma m_0 c^2} A_\theta^2(r, z). \tag{17}$$

This expression for the potential indicates that as far as the $r-z$ coordinates are concerned the particle moves without friction on a surface which is flat except for a 'hilly' region where the elevation is proportional to A_θ^2 (r, z).

Consider a filamentary current ring, which constitutes a simple, physically thin, magnetic lens, for which the square of A_θ is roughly sketched in Fig. 2. There are two poles in the $r-z$ plane where the potential $V(r, z)$ is singular. A particle moving along the z-axis would not be deflected at all. On the other hand a particle moving initially parallel to the z-axis at a radius r_0 would be deflected toward the axis, and would necessarily cross the z-axis at least once. To form a good lens, the amplitude of the magnetic field should be so adjusted that there is only one crossing, at $z = f$, the focal length. We shall see later that, for $r_0 \ll a$, the radial component of velocity imparted to the particle is proportional to r_0, so that f is independent of r_0. However, because the magnetic field $(B_r \hat{r} + B_z \hat{z})$ increases rapidly with radius, the linear relationship does not hold for all $r_0 < a$, and the distance measured along z decreases as r_0 increases. Thus we may say that the focal length of a magnetic lens is a function of the radius $f = f(r_0)$.

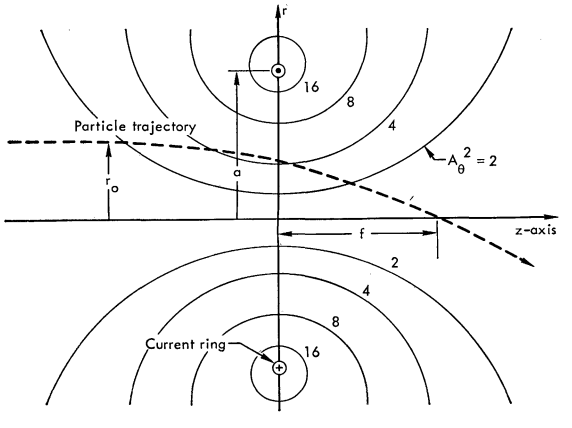

FIG. 2. A sketch of lines of constant A_θ^2 for a simple magnetic lens consisting of a single current ring. A particle moving initially parallel to the z-axis is focused at some point $z = f$ which has a second order dependence on the initial radius r_0.

We can drop the subscript without ambiguity and simply write $f(r)$ for the function characterizing the lens. It turns out that this form of aberration is much larger than that found in optical lenses of comparable physical dimensions.

The magnetic field inside a solenoid is more nearly a constant, and this structure forms a lens in which there is less variation of focal length as we go outward in radius. For the solenoid an approximate formula for the focal length is

$$f^* = 4[H\rho]^2 \Big/ \int_{-\infty}^{\infty} B_z^2 \, dz \tag{18}$$

where

$$H\rho \equiv \beta\gamma m_0 c^2/q \tag{19}$$

determines the particle energy. We have put an asterisk with f to indicate that Eq. (18) is only an approximation, but it is a good one for a long solenoid the length l of which is much greater than the radius a.

For a long solenoid the integral in the denominator of Eq. (18) can be separated into two approximate parts

$$\begin{aligned}\int_{-\infty}^{\infty} B_z^2 \, dz &= 2\left\{\int_0^{l/2} B_0^2 \, dz \right. \\ &\quad \left. + \int_{l/2}^{\infty} \left[\frac{B_0 a^2}{4\pi(z - l/2 + a)^2}\right]^2 dz\right\} \\ &= B_0^2 l + B_0^2 \left(\frac{a}{48\pi}\right)\end{aligned} \tag{20}$$

where the second integral accounting for end effects is negligible if $l \gg a$, so that

$$f^* \approx \frac{4(H\rho)^2}{B_0^2 l}. \tag{21}$$

We note that the vector potential in the interior region of a long solenoid is given by $A_\theta = B_0 r/2$, so that $V(r, z)$ becomes a parabolic mechanical potential $V(r, z) = \frac{1}{2}kr^2$, with $k = q^2 B_0^2/4\gamma m_0 c^2$. A particle starting in this potential at radius r_0 will execute radial oscillations according to the equation

$$r = r_0 \cos \omega t \tag{22}$$

where

$$\omega = \sqrt{k/\gamma m_0} = \frac{qB_0}{2\gamma m_0 c}, \tag{23}$$

or one-half the cyclotron frequency. Thus the radial coordinate of the particle passes through zero periodically. The actual trajectory of the particle is of course a helix, which intersects the z-axis periodically. Alternate loops of the helix are represented by negative values of r in Eq. (22).

The existence of a fringe field at the end of the solenoid does not change the fact that the helix will intersect the z-axis, because this is required by the condition that $p_\theta = 0$. The velocity vector of the particle, after it exits and is far from the solenoid, must again lie in some $r-z$ plane (otherwise p_θ will not be zero). Only if dr/dt is negative will the trajectory again cross the z-axis outside the solenoid.

The solenoid becomes a useful lens if we choose B_0 and the length l such that $\omega T = \omega l/v_z \ll 2\pi$, and $l \gg a$, where a is the radius of the solenoid. This can always be done simply by choosing l large enough and B_0 small enough. In this case, the fraction of one helical loop executed inside the solenoid is small, the change of r near the ends of the solenoid can be neglected, and the velocity component $dr/dt = -r_0\omega \sin\omega T$ will always be negative, and is approximated by

$$\left(\frac{dr}{dt}\right)_{\text{exit}} \approx -r_0\omega^2 T \approx -r_0\omega^2 l/v_z \tag{24}$$

where v_z is the axial component of the particle velocity. The focal length is defined by

$$\frac{(-(dr/dt))_{\text{exit}}}{v_z} = \frac{r_0}{f}, \tag{25}$$

from which

$$f = \left(\frac{4}{B_0^2 l}\right)\left(\frac{\gamma^2 m_0^2 c^2 v_z^2}{q^2}\right) \approx \frac{4[H\rho]^2}{B_0^2 l} \tag{26}$$

assuming $v_z \approx v$, with the equation

$$\frac{\gamma m_0 v^2}{\rho} = \frac{q}{c}(v \times H) \tag{27}$$

determining $H\rho$. Thus, we have derived Eq. (21) by considering the actual particle orbit. If the solenoid is long enough that the end effects can be neglected, the focal length is essentially independent of the radial location of the particle as it passes through the lens.

One objection to an ordinary solenoidal lens, and also to the current ring, is that they both exhibit a dipole moment, and the magnetic field falls off with distance only as fast as that of a dipole. This objection can be removed, however, by providing a cylindrically symmetric iron flux leader to reduce the dipole moment. This procedure is equivalent to providing an auxiliary solenoid outside the primary solenoid to return all of the magnetic flux through the annular area, which eliminates the dipole moment entirely. Either procedure minimizes the spatial extension of the fringe field at the ends, and the focal length is still approximated closely by Eq. (18), provided $l \gg a$.

Even without the problem of the dipole field, space limitations often make it inconvenient to employ a long solenoid, and we wish to consider now the focal properties of some lens structures having axial dimensions not exceeding their radial dimensions.

For these structures Eq. (18) is quite inaccurate, and it is necessary to compute particle trajectories to evaluate $f(r)$. Inspection of several trajectories at different radii allows one to plot a curve of f vs r.

TABLE I (Example 1)

Solenoid	Radius	Length	Current
1	$a+\epsilon$	$l=a$	$-I$
2	$a-\epsilon$	$l=a$	$+1.09297\,I$

We begin with a pair of concentric solenoids in the arrangement described above, with dimensions and currents as listed in Table I. The dipole moments of these two solenoids cancel, i.e., $-(a+\epsilon)^2 + 1.09297\,(a-\epsilon)^2 = 0$, for $\epsilon/a = \frac{1}{45}$, which we choose arbitrarily. The results are of course insensitive to ϵ/a for $\epsilon/a \ll 1$. Here the length is comparable with the radius, so that Eq. (18) would be only approximate. In Fig. 3 we plot the correct focal length, as determined from particle trajectories, in the dimensionless form $F = f(r)/f(0)$ as a function of the dimensionless radius (r/a). We also show the corresponding approximate F^* as determined by integrating $B_z^2\,dz$ over each particle orbit and substituting these values into Eq. (18).

Obviously if optical lenses were as poor in quality as this lens, practically none of the usual applications of lenses would exist. Fortunately a great deal of aberration can usually be tolerated in accelerators before the beam is adversely affected.

Let us now expand the computed focal length f in the series

$$f = \sum_{i=0}^{\infty} f_i \left(\frac{r}{a}\right)^i \tag{28}$$

where f_0 is the nominal focal length (at $r = 0$) and a is the physical radius of the lens. The coefficient f_1 is always zero, and the dimensionless focal length is defined by the equation

$$F = f/f_0 = 1 + F_2(a)(r/a)^2 + \ldots \tag{29}$$

where the coefficient

$$F_2(a) = f_2(a)/f_0 \tag{30}$$

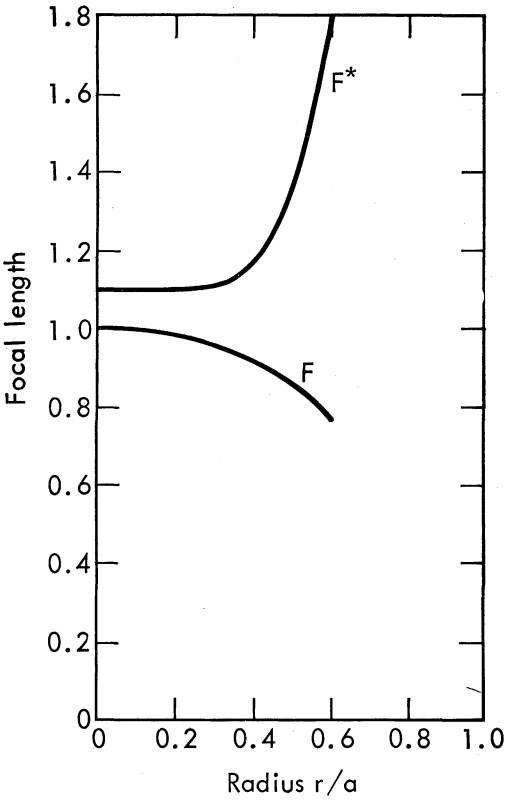

FIG. 3. Curves showing actual focal length F and the approximation F^* as functions of the radius for a lens consisting of two concentric solenoids.

is the second order error in the dimensionless focal length. For our purposes the error $F_2(a)$ will characterize the degree of nonlinearity of a lens.

If we use this expansion for our present example the value of $F_2(a)$ is determined to be -0.64, and we can refer to this as a nonlinearity, or aberration, of 64 per cent, where it is understood that the sign of $F_2(a)$ is always negative. It should be noted that the focal length varies almost parabolically with radius, so that the second order error accounts for nearly all of the aberration that is present.

The approximate function F^* is plotted only for its academic interest, and should not be confused with the second order error in F. There is no special connection between the two functions.

Since we are particularly interested in lenses having the shortest possible axial dimensions, we consider now some structures in which $l \ll a$. For the next example we reduce the concentric solenoids to zero length and consider the extreme case of two concentric rings carrying the currents listed in Table II. As before, the result will be insensitive to ϵ for

TABLE II (Example 2)

Ring	Radius	Axial Position	Ring Current
1	$a+\epsilon$	0	$-I$
2	$a-\epsilon$	0	$+1.09297\,I$

$\epsilon \ll a$, and we take the same value $\epsilon/a = \frac{1}{45}$. For this lens the variation of focal length with radius, shown in Fig. 4, is somewhat more pronounced. The second order error is $F_2(a) = -1.10$, or 110 per cent. The approximate Eq. (18) also yields less accurate results for F^* than in the previous example.

It is important to note that in particular applications of a lens the effective linearity may be improved merely by increasing the physical size of the lens relative to the radius b of the beam being focused. If we expand the normalized focal length in terms of r/b

$$F = 1 + F_2(b)(r/b)^2 + \ldots \tag{31}$$

the second order error

$$F_2(b) = (b/a)^2 F_2(a) \tag{32}$$

relative to the beam size is reduced by the factor $(b/a)^2$, which varies inversely with the square of the lens size.

The magnetic field of our second example is remarkably similar to that produced by existing

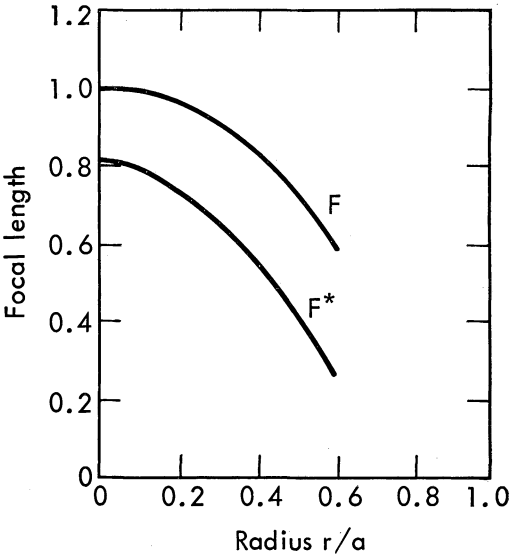

FIG. 4. Focal length curves for the pair of concentric current rings listed in Table II.

focusing magnets of the flux-leader type used extensively in the Livermore Astron Accelerator. After the present calculations suggested the degree of nonlinearity possessed by these lenses, increasing the physical size of certain of the lenses near the leading end of the accelerator (where the beam diameter is largest) by only 50 per cent resulted in an increase of output beam current from approximately 600 A to 850 A.

There is another way to improve the linearity of the two-ring lens without increasing either the radial or the axial dimensions. This method will be illustrated in our final example, which also introduces a type of lens having an 'internal degree of freedom' which actually allows adjustment of the second order error within certain limits.

Before describing this lens we digress briefly to consider multipole expansions of the magnetic field of coaxial current rings. It is particularly important to determine the lowest order multipole required in the expansion for a given lens, because this tells us the general shape of the magnetic field at large distances, and also how rapidly the magnetic field falls off with distance. A good lens should be both physically and magnetically 'thin', and this criterion is placed on a rigorous footing by the following definition:

A thin magnetic lens is generated by a source which can be enclosed within a toroidal surface of major radius a and minor radius ϵ, $\epsilon \ll a$, and the lowest order multipole in the expansion of the magnetic field, convergent outside a sphere of radius $a+\epsilon$, is the octupole.[6]

This definition guarantees thinness of not only the physical structure but the magnetic intensity profile as well, which must fall at least as fast as ρ^{-5}, where (ρ, θ, ϕ) are spherical coordinates ($\rho = 0$ at the center of the torus). The two-ring lens of the previous example satisfies this definition, but the others do not.

We recall that multipole expansions of the electric potential ϕ or the scalar magnetic potential ϕ^* outside a sphere containing the sources (radius $a+\epsilon$) utilize the following moments: Monopole moments ($n = 0$), a scalar, with potential falling off as ρ^{-1}; dipole moment ($n = 1$), a vector, with potential falling as ρ^{-2}; quadrupole moment ($n = 2$), a 3×3 tensor of second rank, potential falling off as ρ^{-3}; octupole moment ($n = 3$), a $3 \times 3 \times 3$ tensor of third rank, potential falling off as $\rho^{-4}, \ldots$, multipole moment (n), a tensor of rank n, with potential falling off as ρ^{-n-1}, with the electric or magnetic field falling off as ρ^{-n-2}.

While the expansion of the electric potential due to a ring of charge has monopole, quadrupole, 16-pole, and higher order multipole moments with even values of n, the scalar magnetic potential of a current ring has only dipole, octupole, 32-pole, and higher order multipoles with odd values of n.

Consider now the net moments of a combination of current rings all centered on the z-axis, but not necessarily concentric. The dipole moments of two rings having equal and opposite dipole vectors ($a_1^2 I_1 = -a_2^2 I_2$) will cancel regardless of the relative axial positions (z_1, z_2) of the two rings. This pair will in general exhibit a quadrupole moment, however, unless the two rings are at the same axial position. A quadrupole moment generated because $z_1 \neq z_2$ can be cancelled by any other pair of current rings $(a_3, z_3, I_3;\ a_4, z_4, I_4)$ having the same quadrupole moment except for sign, so that

$$a_4^2 I_4 z_4 - a_3^2 I_3 z_3 = -(a_2^2 I_2 z_2 - a_1^2 I_1 z_1). \qquad (33)$$

We can solve this equation by imposing configurational symmetry about the plane $z = 0$, and requiring that $a_3^2 I_3 = -a_4^2 I_4$. We obtain $a_3 = a_1$, $a_4 = a_2$, $z_3 = -z_1$, $z_4 = -z_2$, $I_3 = I_1$, $I_4 = I_2$, and $I_2 = -(a_1^2/a_2^2) I_1$. It is important to note that if the dipole vectors of rings 1 and 2 point toward each other, the dipole vectors of rings 3 and 4 must point away from each other in order to change the sign of the quadrupole tensor. The lowest order moment remaining is then the octupole moment.

It is now clear that the previous example (two-ring lens) is not the most general magnetic field satisfying our definition of a thin lens. Any number of current rings can be placed inside the toroidal surface containing the sources of the field so long as the dipole moments and quadrupole moments are selected to cancel. The far field ($\rho \gg a+\epsilon$) then will involve at most an octupole component; yet the near field ($\rho < a-\epsilon$) can be designed to have a variety of patterns depending on the number of rings employed.

The problem is to find a set of current rings, or more generally, a current density distribution $j_\theta(r, z)$ inside the bounding torus that will minimize the second order error in focal length.

We shall not formally minimize the second order error for a thin lens, but instead we show how to reduce it substantially from that of the foregoing example to a value which we believe cannot be improved upon significantly. To do this we note that the magnetic intensity $B_z(r, 0)$ in the two-ring lens of Example 2 is positive, and increases somewhat with r as we approach the inner ring. On the

other hand the four-ring configuration listed in Table III, which represents two equal quadrupoles of opposite sign, or a new octupole, produces a negative axial component of magnetic field in the plane $z = 0$, which also increases in intensity as we approach Ring 4. A superposition of the old and the new octupoles results in a net field component $B_z(r, 0)$ which is almost independent of the radius over a substantial range. In this respect the field behaves somewhat like that of a long solenoid.

TABLE III (Example 3)

Ring	Radius	Axial Position	Current
3	$a+\epsilon$	0	$-18.5339\,I$
4	$a-\epsilon$	0	$-18.5339\,I$
5	a	ϵ	$18.5430\,I$
6	a	$-\epsilon$	$18.5430\,I$

Our final example then consists of a total of six current rings (1, 2, 3, 4, 5, 6), as listed in Tables II and III, and the level of current in the four rings producing the new octupole component (3, 4, 5, 6) can be set independently of the level of current in the original pair (1, 2) producing the old octupole component. If the new octupole component is zero we regain the result of Example 2 (110 per cent). However, as we increase the amplitude of the new octupole component the second order error is reduced until it reaches a minimum, and then it increases. We have actually listed in Table III the level of current corresponding to this minimum. The corresponding focal length is plotted in Fig. 5, and the second order error is $F_2(a) = -0.56$, or only 56 per cent. This represents the most perfect thin lens we have been able to devise.

The really significant point to note is that the aberration in this particular thin lens is less than that in the solenoidal lens of length $l = a$, where the error was 64 per cent.

It should be observed that two of the current rings in this example are redundant, because rings 1 and 3, and also rings 2 and 4, coincide. Two of the rings, say 1 and 2, can therefore be removed if the currents which they carry are transferred to the remaining rings. We then have a relatively good, practical four-ring adjustable lens free of iron.

We note that the new octupole component in this example could equally well be generated by four rings of equal radius located at $z = -\epsilon, 0, 0, +\epsilon$, and carrying $+, -, -, +$ currents, respectively.

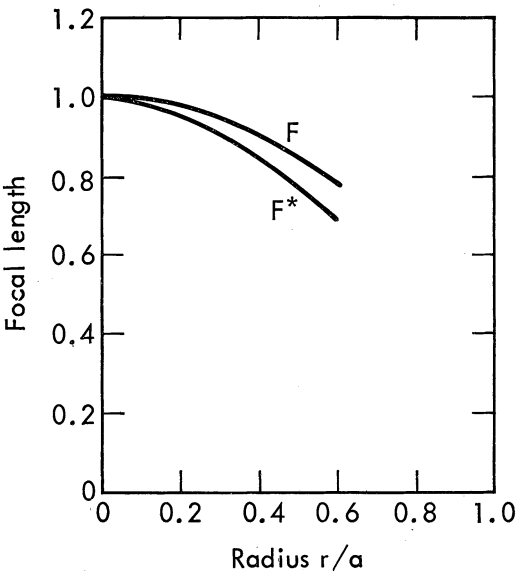

FIG. 5. Focal length curves for a four-ring lens for which the aberration is adjustable.

This configuration represents two linear quadrupoles 'back to back'. Since there would be identical current rings at $z = 0$ [carrying a total current of $-2(18.5430)I$] the final lens would require a total of five rings, and the two linear quadrupoles are in this case independent of the old concentric ring quadrupole.

One could also add, as a further refinement of the local field, a set of eight rings of equal radii at $z = -\epsilon, -\epsilon/2, -\epsilon/2, 0, 0, \epsilon/2, \epsilon/2, \epsilon$ forming two octupoles back to back. The currents would be equal, and would follow the pattern $+ - - + + - - +$ with respect to sign. A total of five physical rings would be required for this 16-pole configuration, and so on.

It may be possible to design a lens involving a single current ring partially clad with iron which will be as 'good' as the lens of Example 3. However it would not be as thin physically, and the error would not be adjustable.

From the foregoing considerations it is clear that the nonlinear focal property is present to a greater or lesser degree in every lens. If the problem of aberration is alleviated by increasing the physical size, the fringe field begins to reach further and further, and may eventually affect other apparatus in the accelerator. In any case it is a costly procedure which may increase the overall size of the machine beyond acceptable limits. It therefore becomes important to determine in particular

applications how much aberration can be tolerated, so that the minimum size of lens, consistent with good beam quality, can be utilized.

4. TRANSPORT OF COMPENSATED HIGH-CURRENT BEAMS THROUGH NONLINEAR LENSES

It is clear that translational symmetry in beam transport is generally broken by lens aberration. However, we now show that a symmetric pattern of laminar flow periodic in z can still be realized by matching the radial distribution of beam current to the lens nonlinearity, provided the aberration is not excessive. A 'hollow' beam is required in the sense that the current density $j(r)$ must increase with r. A criterion is derived for determining when the aberration is too excessive to allow correction of the difficulty with a beam compensated in this way.

We begin the problem with a given lens function $f(r)$, and assume that all of the lenses in the periodic structure are characterized by this function.

We can arrange for periodic laminar flow in the following way: Let us consider a concentric tube of beam flux contained within a particular shell of radius R_s with minimum radius R_n halfway between lenses and maximum radius R_x at each lens. The current transported by this tube $I(R_x)$ increases as we go outward in R_x, but not necessarily as R_x^2. Note that the maximum values of R_n, and R_x, and $I(R_x)$ are just $R_{\min}$, $R_{\max}$, and I respectively. The quantity A likewise becomes a function of R_x: $A = A(R_x)$. We can now rederive Eq. (10) just as we did before, but using these new variables and the differential equation

$$\mathrm{d}^2R_s/\mathrm{d}z^2 = A^2(R_x)/R_s. \tag{34}$$

The nonlinear property of the lenses is specified by

$$2\frac{\mathrm{d}R_s}{\mathrm{d}z} = R_x/f(R_x) \tag{35}$$

analogous to Eq. (7). In determining the shape of a particular shell $R_s(z)$, we hold R_n, R_x, $I(R_x)$, and A constant with respect to z. Then in the final equation analogous to Eq. (10) we have

$$\frac{Z}{f(R_x)} = 8\alpha \exp(-\alpha^2)\,\Phi(\alpha) = g\left(\frac{R_x}{R_n(R_x)}\right) \tag{36}$$

where now $R_n(R_x)$ must be regarded as a function of R_x, and where the functions

$$\alpha(\mu) = [\ln(R_x/R_n(R_x))]^{1/2} = (\ln\mu)^{1/2} \tag{37}$$

and $g(\mu)$ are also related to R_x through the defining Eq. (8) or (37) for μ. For uniform beams transported through perfect lenses the ratio R_x/R_n is independent of R_x, but this is not true here, and in fact Eq. (36) can be used to determine $\alpha(R_x)$ since we already are given the left-hand side $Z/f(R_x)$ as a function of R_x. Having determined $\alpha(R_x)$ we can then use the analog of Eq. (4) to determine $A(R_x)$. We obtain

$$A(R_x) = \sqrt{2}\left(\frac{R_n}{R_x}\right) R_x \int_0^{\alpha} \exp(t^2)\,\mathrm{d}t \tag{38}$$

and from Eq. (2)

$$I(R_x) = \frac{m_0 c^2 \beta^3 \gamma^3}{2q} A^2(R_x) \tag{39}$$

$$\mathrm{d}I = 2\pi R_x j(R_x)\,\mathrm{d}R_x \tag{40}$$

$$j(R_x) = \frac{1}{2\pi R_x}\frac{\mathrm{d}I(R_x)}{\mathrm{d}R_x} \tag{41}$$

which is the current density required for laminar flow.

As we consider various shells lying further and further out from the axis (R_x increasing) we note that the left-hand side of Eq. (36) generally increases. From Fig. 1 we see that this requires an increase in α and μ, and consequently an increase in the current density $j(R_x)$ as we go outward. However, since we are increasing both R_x and the ratio R_x/R_n, it is important to avoid a situation in which R_n must decrease in order to make the ratio R_x/R_n increase, for this could be realized only by nonlaminar flow. It is easy to derive a criterion which will guarantee that we do not encounter this situation. We simply require that $\mathrm{d}R_n/\mathrm{d}R_x$ be positive in the equation

$$\frac{Z}{f(R_x)} = g\left(\frac{R_x}{R_n}\right) = g(\mu). \tag{42}$$

We differentiate this equation to find

$$-\frac{Z[\mathrm{d}f/\mathrm{d}R_x]\,\mathrm{d}R_x}{f^2} = \frac{R_n\,\mathrm{d}R_x - R_x\,\mathrm{d}R_n}{R_n^2}\frac{\mathrm{d}g}{\mathrm{d}\mu}, \tag{43}$$

or

$$\frac{\mathrm{d}R_n}{\mathrm{d}R_x} = \frac{R_n}{R_x}\left\{1 + \frac{R_n(\mathrm{d}f/\mathrm{d}R_x)Z}{f^2(\mathrm{d}g/\mathrm{d}\mu)}\right\}. \tag{44}$$

This will be a positive quantity if and only if the quantity in brackets is positive, which requires that the inequality

$$-\left(\frac{df/f}{\mathrm{d}R_x/R_x}\right) < \left(\frac{R_x}{R_n}\right)\frac{1}{g}\left(\frac{\mathrm{d}g}{\mathrm{d}\mu}\right) \tag{45}$$

be satisfied. Since $g(\mu)$ is simply the ordinate in

Fig. 1, we can determine $(1/g)\,(\mathrm{d}g/\mathrm{d}\mu)$ either graphically or from the expression

$$g(\mu) = 8\sqrt{\ln\mu}\,\frac{1}{\mu}\int_0^{\sqrt{\ln\mu}} \exp(t^2)\,\mathrm{d}t. \tag{46}$$

It is then easy to apply the criterion to any lens function f.

In practice it is probably difficult to form a hollow beam having a precisely specified current density distribution. However, if the beam is merely 'somewhat hollow' it may be possible using lenses with an internal degree of freedom, as in Example 3, to adjust the lens nonlinearity to 'match' such a beam to second order, and in this way obtain better results than if the beam were uniform.

5. TRANSPORT OF UNIFORM BEAMS THROUGH NONLINEAR LENSES

It is important to determine how much aberration of the type described above can be tolerated in the transport of uniform high current beams of the type considered in Sec. 2. Where the lens focal length varies with radius it is essentially impossible to treat the transport of uniform beams analytically. Even if a beam starts with uniform density over the cross section it generally does not remain uniform because of the nonlinearity.

Assuming axially symmetric flow it is easy to see why a strong nonlinearity may alter an otherwise uniform current density. This can happen when a group of particles originally lying near the outer edge of the beam is focused too strongly and begins crossing the trajectories of other particles. The inner particles normally do not experience the electric and magnetic fields of the outer particles, but if the trajectories begin to cross (in $r-z$ space) this role is reversed, and deterioration of the pattern of laminar flow results. The two-stream instability (in the radial direction) becomes possible.

The usual matrix methods for beam transport are not applicable where the beam is in a nonlinear dynamical state. However, a numerical calculation allows one to carry the beam through successive lenses by taking steps along z which are much smaller than the lens spacing.

The numerical procedure divides the circular beam in its initial state up into n concentric shells with the ith shell carrying current I_i, and the total current I given by

$$\sum_{i=1}^{n} I_i = I. \tag{47}$$

During transport through the lenses these shells remain centered on the z-axis, but they are allowed to cross in $r-z$ space. In contrast with laminar flow the radial ordering of shells can change as we move along in z. One of the effects of strongly nonlinear lenses is finally to bring the outermost shell all the way to the inside where it becomes an inappropriately located shell carrying quantities of charge and current which are excessive for that location.

The shells are assumed initially to have equal thickness, so that the current carried in the ith shell is proportional to i. The differential equation for the trajectory of the ith shell is thus

$$\mathrm{d}^2 r_i/\mathrm{d}z^2 = \frac{A^2}{r_i}\cdot\frac{1}{I}\sum_{r_j<r_i} I_j, \tag{48}$$

where, because of axial symmetry, the ith shell 'sees' only these shells having radii less than r_i. If we set

$$I_i = ki \tag{49}$$

where k is a constant, we have

$$I = \sum_1^n ki = k\frac{n}{2}(1+n) \tag{50}$$

from which

$$k = \frac{2I}{n(n+1)}. \tag{51}$$

Then the equation for the ith trajectory becomes

$$\mathrm{d}^2 r_i/\mathrm{d}z^2 = \frac{2A^2}{n(n+1)}\cdot\frac{1}{r_i}\sum_{r_j<r_i} j \tag{52}$$

where the summation is taken over those values of j for which $r_j < r_i$.

Conventional methods of numerical integration are used to perform the integration of the n equations step-wise with respect to z. On reaching a lens the quantity $r_i/f(r_i)$ is subtracted from each $\mathrm{d}r_i/\mathrm{d}z$ to simulate passage of all shells through the lens. The lens function $f(r)$ must be prescribed.

If the lenses are selected and placed according to the prescription given in Section II, and if they are all linear, then laminar flow is maintained in the shell model. In fact, the trajectory of each shell can be calculated exactly by the methods of Section II. In a phase-space diagram for this sort of ideal transport, the representative points for the different shells lie in a straight line, as shown in Fig. 6. In going from one lens to another the outer shell moves along the curve from B to A; at each lens it jumps

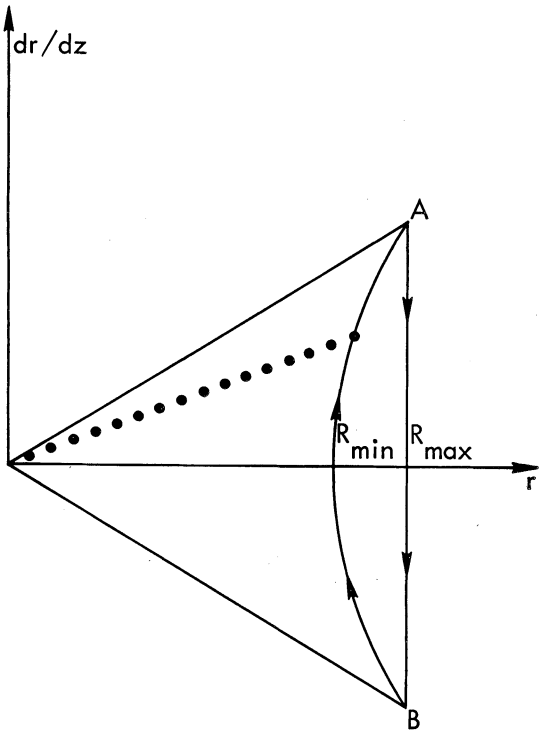

FIG. 6. Phase-space diagram, drawn for a particular position z, for a beam periodic in z being transported through linear lenses. Each dot represents a shell, and the arrows indicate the path followed by the outer shell as it moves along in z.

from A to B. The fact that all of the representative points execute trajectories in phase space similar to that of the outer shell is responsible for maintaining the points in a straight line.

Upon introducing a nonlinear lens function $f(r_i)$, the straight line of representative points becomes immediately distorted after passage through the first lens. Since $f(r_i)$ decreases with r_i the outer shell jumps from A down to some point B' somewhat below B. Just after exit from the lens the representative line in phase space is curved downward. With this situation the passage to the next lens can not be expected to carry the outer shell back to the original point A, but to a new point A' which is typically above A, etc.

Consider now a specific example which illustrates this type of behavior. We normalize all linear dimensions to the minimum beam radius, $R_{\min}$, and consider a (high-current) beam with current and energy such that $A^2 = 0.01$, which in the absence of lens aberration would be in periodic, laminar flow, with $R_{\min} = 1.0$, $R_{\max} = 1.122$, $Z = 10.0$, and $f(0) = 11.673$. For the lens function we take

$$f(r) = f(0)\left[1 - 0.30\left(\frac{r}{R_{\min}}\right)^2\right],$$

implying that the second order error $F_2(R_{\min})$ is 30 per cent. If we now follow the shell model numerically employing 200 shells, with the starting condition for the lens of representative points at $z = 0$ as shown in Fig. 7(a), we find that passage through the first lens (exit lens 1) merely bends the line downward slightly. This bending increases somewhat as the beam is transported through successive lenses, but the original ordering of shells is retained, indicating that the flow remains

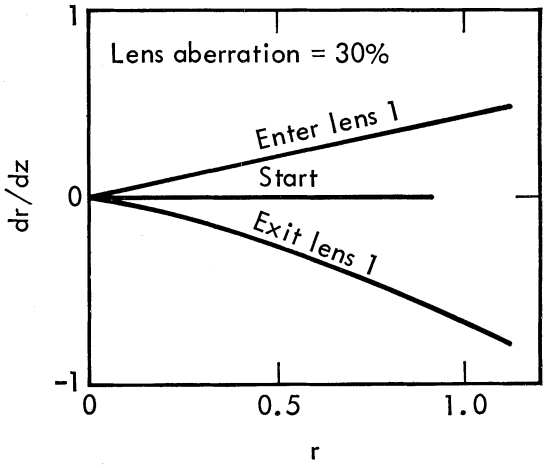

(a)

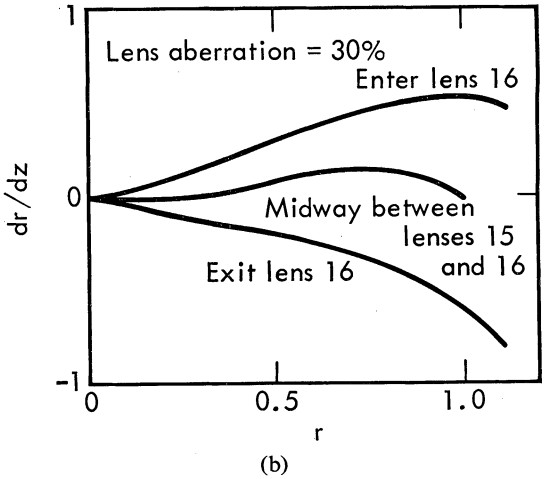

(b)

FIG. 7. Phase-space diagrams illustrating beam transport through periodic nonlinear lenses in which the aberration $F_2(R_{\min})$ is 30 per cent. The flow is still laminar at the 16th lens.

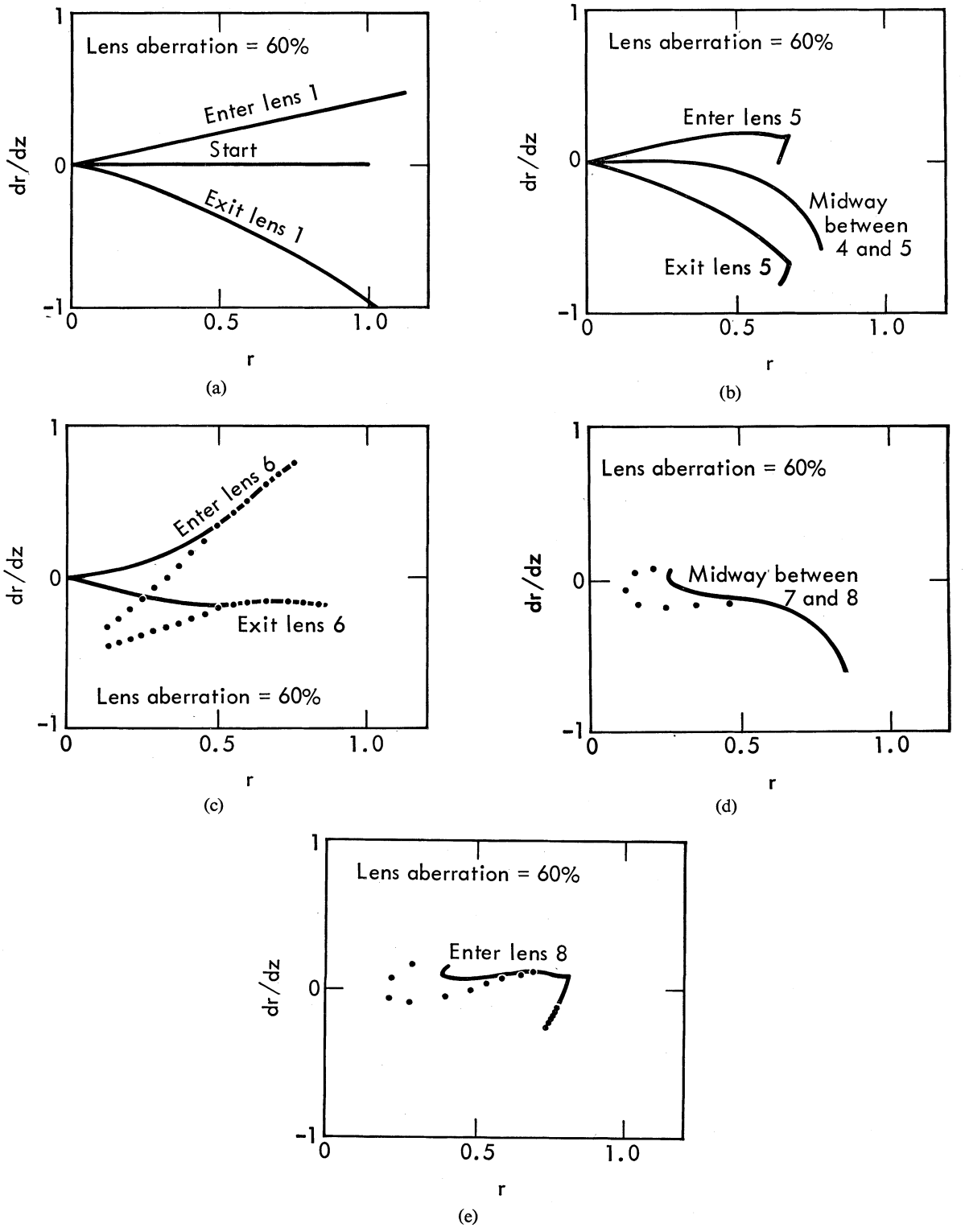

FIG. 8. Phase-space diagrams showing breakdown of laminar flow when the lens aberration is 60 per cent.

laminar. At the 16th lens, the pattern of flow, shown in Fig. 7(b), suggests that the current density is still reasonably uniform after passage through many lenses.

If we use the same beam, however, and repeat the calculation with the lens aberration increased to 40 per cent, there is a distinct break in the pattern of laminar flow at the 12th lens. Increasing the aberration to 50 per cent upsets the laminar flow by the time we reach the 8th lens, and increasing it to 60 per cent moves the breakpoint up to the 5th lens.

Figure 8 illustrates how the pattern of flow is disturbed when the aberration is 60 per cent. In Fig. 8(a) there is a substantial difference between the entry and exit conditions at the first lens. In Fig. 8(b) there is severe bending (compression of the outer shells) halfway between the 4th and 5th lenses, and the first crossing of shell trajectories is found at the entrance to lens 5. Here there is sufficient radial spread to identify several individual shells. By the time lens 6 is reached the outer shells that had gone out of order have come into a smaller radius and also spread in radius essentially over the whole range occupied by the original beam. In Fig. 8(d) one sees how the excessive charge associated with the original outer shells drives the 'weak' inner shells outward, thus perturbing a portion of the beam which otherwise would not have been perturbed significantly by the lens aberration alone. At the 8th lens (Fig. 8(e)) the beam has a distinct hole in the center, and a new group of shells is being thrown into an inverted order.

Although the beam thereafter remains hollow to the extent indicated in this last figure, it continues to be transported, in spite of considerable phase-space mixing, without going outside the limit $r = 1$. However, the 'average' phase-space density is reduced because of the mixing, and the beam quality is therefore somewhat poorer. Nevertheless, our conclusion is that a surprising amount of aberration can be present before the beam quality is affected significantly.

6. SUMMARY

We have treated the problem of transporting a high-current coasting beam through discrete magnetic lenses. A beam envelope periodic in z is easily realized in the case of linear lenses by appropriate choice of the spacing and focal length. Accelerated beams can be similarly transported, but the system in this case is generally aperiodic.

We have found that practical lenses have a large amount of aberration when compared with optical lenses of the same size. The focal length is longest for particles at the center of the beam and shortest for those at the edge.

Periodic transport of a coasting beam through nonlinear lenses is possible if the beam is carefully hollowed out (compensated) to match the lenses. We have shown how a lens can be arranged to permit internal adjustment of the nonlinearity to aid in this matching.

Finally we have found that moderate amounts of lens aberration may be allowed before an uncompensated beam becomes hollow of its own accord, or exhibits any other loss of quality such as brightness.

REFERENCES

1. Electron accelerators capable of producing more than a million amperes at 10 MeV energy are now commercially available.
2. N. C. Christofilos and T. K. Fowler, 'Proposal for Extension of the Astron Accelerator to 6 MeV,' University of California, Lawrence Radiation Laboratory, Report No. 50355, (1968).
3. M. L. Andrews, H. Davitian, D. A. Hammer, H. H. Fleishmann, J. A. Nation, and N. Rostoker 'On the Propagation of High-Current Beams of Relativistic Electrons in Gases,' *Appl. Phys. Letters*, **16,** No. 3, 98 (1970).
4. C. H. Woods, 'The Image Instability in High-Current Linear Accelerators,' *Rev. Sci. Instr.* **41,** 959 (1970).
5. N. W. Hetherington and C. H. Woods, 'The Effects of Space Charge and Relativity on the Shapes of Charged Particle Beams,' University of California, Lawrence Radiation Laboratory, Report No. 6010 (1960).
6. We consider in this paper only axially symmetric systems. For other types of lenses, used primarily for low-current, information-carrying beams, see P. W. Hawkes, *Quadrupoles in Electron Lens Design* (Academic Press, 1970).
7. Two of these current rings form a linear quadrupole (related to the spherical harmonic function Y_{02}) while the quadrupole magnets often used in high-energy particle accelerators form a planar quadrupole (Y_{22}). [See for example Philip M. Morse and Herman Feshbach, *Methods of Theoretical Physics* (McGraw-Hill Book Company, Inc. 1277.] Neither of these should be confused with the two-ring 'quadrupole' or the four-ring 'octupole' employed in torroidal plasma confining devices, so called because they generate approximately a two-dimensional multipole field in the region of confinement. (See for example Ref. 8.)
8. T. Ohkawa, M. Yoshikawa, and A. A. Schupp, 'Plasma Instabilities in Gulf General Atomic Multipole Devices,' *Plasma Physics and Controlled Nuclear Fusion Research II*, (1968) p. 321.